A comprehensive Holocene sediment budget for the Ganges-Brahmaputra-Meghna river delta

By

Jessica Lynn Raff

Thesis

Submitted to the Faculty of the

Graduate School of Vanderbilt University

in partial fulfillment of the requirements

for the degree of

MASTER OF SCIENCE

in

Earth and Environmental Science

August 9, 2019

Nashville, Tennessee

Approved:

Steven L. Goodbred Jr., Ph.D.

John C. Ayers, Ph.D.

To my parents, for their unconditional love and support

ACKNOWLEDGMENTS

Funding support for this research was provided by National Science Foundation (NSF) award number OCE1600319. I also received support from Vanderbilt's University Graduate Fellowship. This work would not be possible without the former and current members of the Goodbred Lab, who analyzed so many of the samples used within the BanglaPIRE database and in this work specifically. I would like to specially acknowledge Rachel Bain and Dr. Elizabeth Chamberlain for their help and feedback throughout this project. The support and guidance of my advisor, Dr. Steve Goodbred, has helped me grow as a scientist. I am thankful for his encouragement to pursue interesting workshops, research directions, and professional development experiences throughout my time in graduate school. I am also appreciative of the feedback and insights that my committee members, Dr. John Ayers and Dr. Dan Morgan, provided throughout the research and writing process. The welcoming community of students, faculty, and staff in the Earth and Environmental Sciences Department has made my graduate school experience truly memorable. Last, but not least, I would like to acknowledge my friends and family for supporting me during this project.

TABLE OF CONTENTS

LIST OF TABLES

LIST OF FIGURES

Chapter 1

Introduction

1.1 Motivation

Recent rates of sea-level rise for Bangladesh range from <3 mm·yr^{-1} to $\sim$8 mm·yr^{-1} based on tide gauge data (Karim and Mimura, 2008; Pethick and Orford, 2013; SMRC, 2003). As a composite system, portions of the Ganges-Brahmaputra-Meghna river delta (GBMD) are in "maintenance" or "construction" phases, meaning that they are either not losing land or may be building or prograding (Fig. 1.1; Wilson and Goodbred Jr., 2015). However, portions of the delta are in a "destruction" phase and experiencing erosion and land loss due to a combination of sea-level rise, subsidence, and insufficient sediment supply (Allison, 1998; Wilson and Goodbred Jr., 2015). Bangladesh, and the GBMD more generally, is expected to experience climate change in the form of increased but more variable monsoon rainfall (e.g. Turner and Annamalai, 2012) and rising temperatures (potentially up to a 2.6°C increase in Bangladesh over the next $\sim$50 years; e.g. Ahmed and Alam, 1999; Karim and Mimura, 2008). Short-term flooding from cyclones and storms (e.g. Karim and Mimura, 2008; Wilson and Goodbred Jr., 2015) and inundation from sea level rise pose a risk not only for the GBMD, but also for the $>$160 million people who inhabit the delta. Wilson and Goodbred Jr. (2015) identify that the areas of the delta in "decline" (*i.e.* losing land and/or elevation) are likely those most at risk to the effects of climate change. In addition, existing literature on human-altered "poldered" regions of the coastal delta demonstrate these heavily-populated regions often see high rates of both subsidence and inundation/flooding (e.g. Allison, 1998; Pethick and Orford, 2013).

To fully understand changes occurring along the GBMD, it is necessary to understand the delta's sediment budget: mass inputs, sediment delivery, and depocenters. The first detailed sediment budget for the delta (Goodbred Jr. and Kuehl, 1999) showed that of the $>1\text{x}10^9$t·yr^{-1} of sediment delivered to the delta from its rivers, $\frac{1}{3}$ was deposited subaerially while the rest of the load

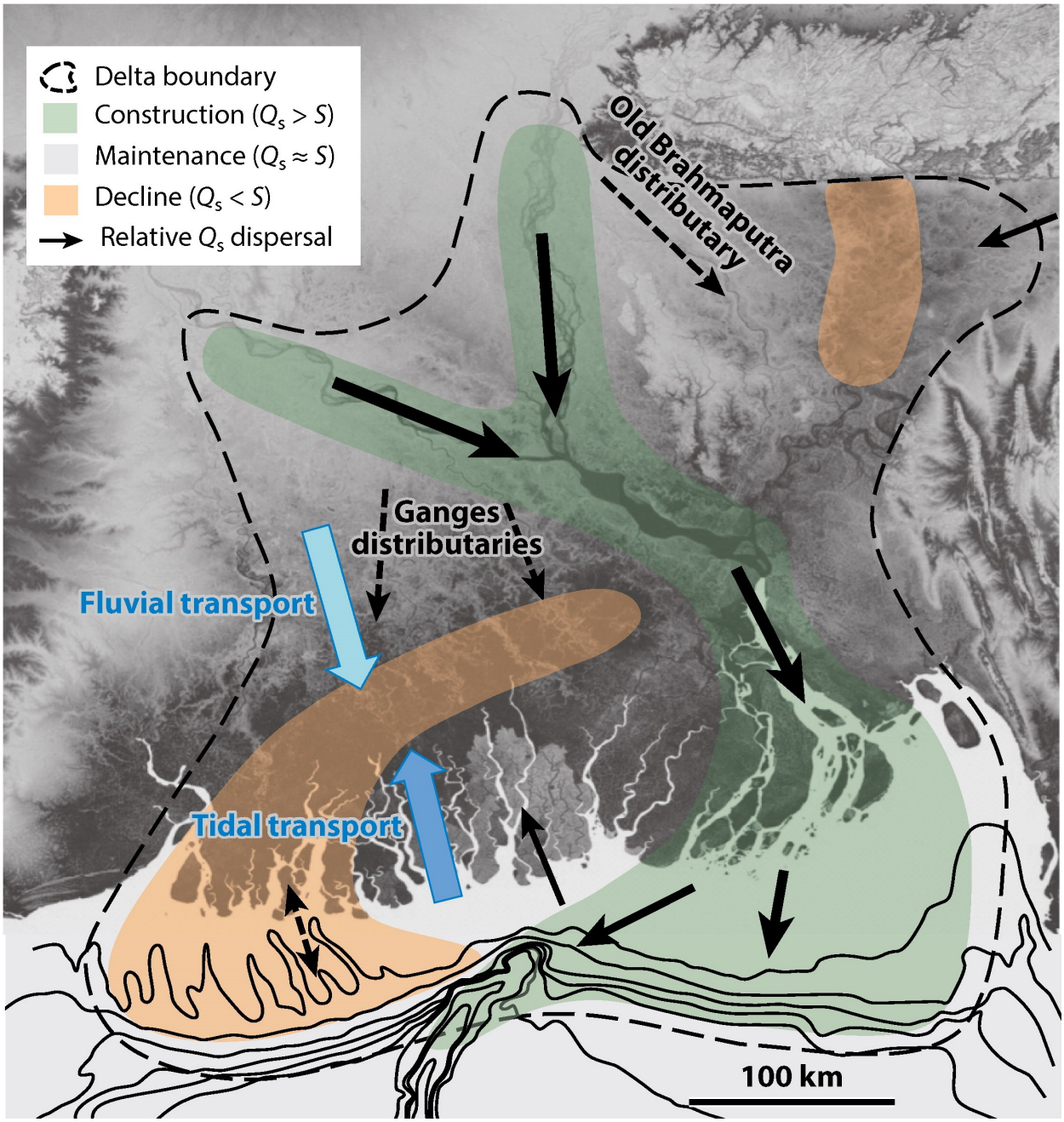

Figure 1.1: Growth and decline of the Ganges-Brahmaputra-Meghna river delta from Wilson and Goodbred Jr. (2015). The delta is experiencing construction and growth along the river paths of the modern Ganges and Brahmaputra rivers where the rate of sediment supply (Q_s) exceeds the rate of subsidence (S). Sylhet Basin and the western tidal delta are experiencing decline because the sediment supply is insufficient to keep pace with regional subsidence rates. The rest of the delta is stable.

was deposited offshore or in the deep marine sink (Kuehl et al., 1989, 1997; Wilson and Goodbred Jr., 2015). In addition, Goodbred Jr. and Kuehl (2000) demonstrated that the the GBMD's sediment budget appeared to be twice as large in the early Holocene Epoch from *ca.* 11,000-7,000 yrs BP compared to modern and mid-late Holocene estimates of sediment discharge. A likely cause for this increased early-Holocene sediment delivery is a concurrent increase in the strength of the Indian Summer Monsoon (ISM; Sandeep et al., 2017; Goodbred Jr. and Kuehl, 2000, and the references cited therein). The work by Goodbred Jr. and Kuehl (1999) provides the existing sediment budget for the GBMD (as a whole), although recent studies have focused on understanding the details of fluvial morphodynamics and delta development over the Holocene (e.g. Goodbred Jr. et al., 2014).

This study seeks to expand the work of Goodbred Jr. and Kuehl (1999, 2000) and Goodbred Jr. et al. (2014), among others, to develop a detailed sediment budget for the Holocene GBMD using a database of >400 cores, >4,500 sediment samples, >150 radiocarbon samples, and bulk geochemical data. This study aims to place GBMD growth and evolution in the context of changes in climate, sea level, and sediment supply. The stratigraphic record of the GBMD and a mass-balance framework will be used to link changes occurring within the delta (and preserved in the record) to those occurring in source terrains (*i.e.* Himalayas) or to allogenic processes over the last 12,000 years. This work will supplement our understanding about the fate of the GBMD, providing insights into historic and modern sediment depocenters and transport paths of the sediment supply (Michael et al., 2013). In addition, this research may provide an analog to anticipated changes in both autogenic/allogenic forcings and delta response in a changing climate.

1.2 Introduction to river deltas

Coastal river deltas develop where sediment-laden rivers enter the ocean and are major depocenters for sediment as it moves through a fluvial system (e.g. Galloway, 1975; Milliman and Syvitski, 1992). Deltas provide ecosystem services such as agricultural land or supplies of freshwater (e.g. Renaud et al., 2013), and as such, much of the literature focuses on river deltas in the

context of humans: benefits, concerns, and human modifications to the delta. Recent studies suggest that some river deltas in their current state are so heavily influenced by humans, they have entered an "anthropocene" level of modification (Giosan et al., 2014; Renaud et al., 2013). Human activities like groundwater or natural gas extraction have exacerbated subsidence and damming has decreased sediment supply, ultimately making deltas vulnerable to flooding and inundation, and potentially drowning (e.g. Syvitski et al., 2009; Giosan et al., 2014; Blum and Roberts, 2009). Sea-level rise scenarios indicate some deltas, like the Danube, could face a loss of 80% of delta land over the next 80 years (Giosan et al., 2014). Similarly, the Mississippi Delta has already lost significant wetland area and it is anticipated that an additional $\sim$10,000 km^2 of land area will become permanently inundated by the end of the century (Blum and Roberts, 2009).

River delta morphology develops as a result of the interplay between wave, tide, and fluvial processes (Galloway, 1975). In the classical "Galloway" framework for delta description, deltas are classified as wave-dominated (*i.e.* Sao Franciso river delta, Brazil), tide-dominated (*i.e.* Fly river delta, Papua New Guinea), or river-dominated (*i.e.* Mississippi river delta, USA) based on morphology (Galloway, 1975). Some deltas exhibit mixed morphology and are classified accordingly [Fig. 1.2; *i.e.* mixed wave-tide influenced (Ebro river delta, Spain), wave-river influenced (Mekong river delta, Vietnam)]. In these mixed system examples, the Ebro river delta displays morphology characteristic of both wave- and tide-dominated systems and the Mekong river delta displays morphology characteristic of both wave- and river-dominated delta systems. Delta growth and behavior is often system-specific due to the unique combination of mass inputs, boundary conditions, and relative influences of wave, tide, and fluvial processes. Delta resiliency, in terms of the ability of the delta to withstand potentially detrimental effects of external forcing mechanisms (e.g. Gersonius et al., 2016), may vary based on factors such as sediment supply, elevation, and subsidence rates. Although deltas like the Danube may lose over $\frac{3}{4}$ of total delta area, predictions for several other deltas are on the order of 5-30% of land area (Giosan et al., 2014). Research into delta risk and sustainability must be targeted for the particular system of interest to fully capture how anthropogenic and natural processes influence delta resiliency.

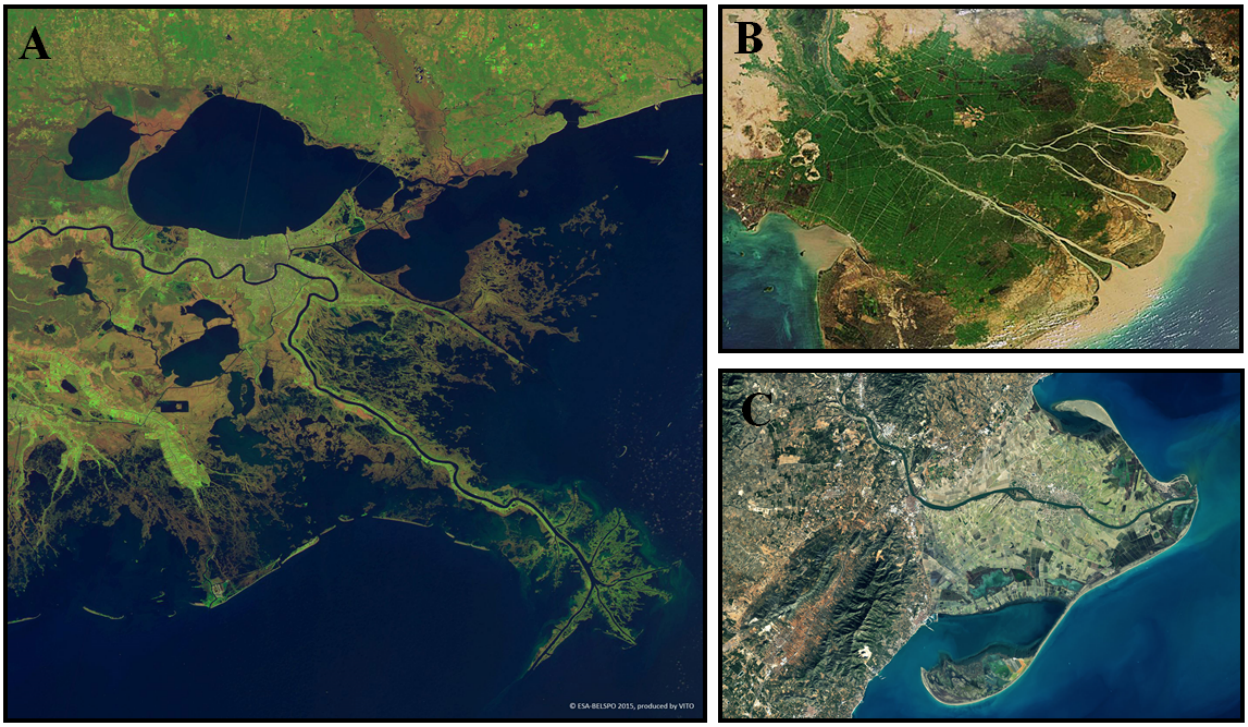

Figure 1.2: Examples of delta morphology and classification. A) River-dominated Mississippi river delta, USA. This southern portion of this delta contains the ”bird-foot” shape characteristic of a river-dominated delta and some mouth-bar deposits are visible (Galloway, 1975). Image from ESA Earth Online 2015. B) Tide-influenced Mekong river delta, Vietnam. Tide-influenced deltas are often characterized by islands separated by sinuous tidal channels (Galloway, 1975). Image from the Dutch Water Sector (2012). C) Wave-influenced Ebro river delta, Spain. Wave-influenced deltas often form spits, barrier-islands, and beach ridges (Galloway, 1975). Image from Taylor et al. (2018), NASA Earth Observatory.

Deltas are archives of landscape evolution, but it may be difficult to decipher signals in the stratigraphic record. In most deltas, a single river draining a mountainous source terrain enters the oceans and deposits sediment along the river path, forming a so-called ”delta lobe”. The lobe forms from crevasse splays, overbank flooding, and river mouth deposition (e.g. Allison et al., 2003; Day et al., 2007). The delta will prograde along the lobe while the river occupies that channel, but when the river avulses, a new lobe will begin to develop (e.g. Allison et al., 2003; Day et al., 2007). The river may revisit older lobes and this may lead to stacking and mixing of lobe deposits within delta stratigraphic records. The history of lobe development and delta growth is well understood for some deltas, like the Mississippi (e.g. Day et al., 2007), but is less evident

in others like the Ganges-Brahmaputra-Meghna river delta (e.g. Allison et al., 2003; Day et al., 2007). To understand delta history and future change, researchers study delta lobes and stratigraphy with widespread sediment coring, mineralogical and geochemical analyses, stratigraphic reconstructions, and sediment dating.

1.3 Background

1.3.1 Geologic setting

The GBMD is a tide-dominated delta (Galloway, 1975) located in southeast Asia that encompasses Bangladesh and part of India (Fig. 1.3A). It is one of the largest river deltas in the world (e.g. Wilson and Goodbred Jr., 2015) and has an area >120,000 km^2 (Wilson and Goodbred Jr., 2015). Active tectonics strongly influence the eastern half of the delta, which is bordered by the Shillong Plateau along several thrust faults to the northeast and the Tripura Fold Belt (in the Indo-Burman Ranges) in the east (Grall et al., 2018). The western portion of the delta (the Indian Shield; Allison, 1998) is part of the Indian craton. This region is comparatively less tectonically active than the eastern delta, but experiences moderate subsidence on the order <1.5 $mm{\cdot}yr^{-1}$ (Grall et al., 2018) and there is evidence for tectonic activity from uplifted Pleistocene terrains such as the Barind Tract (Fig. 1.3; e.g. Morgan and McIntire, 1959; Grimaud et al., 2017; Pickering et al., 2018). Subsidence rates across the delta increase moving from the delta apex towards the offshore (>5 $mm{\cdot}yr^{-1}$; Grall et al., 2018; Reitz et al., 2015), with the exception of Sylhet Basin (Fig. 1.3B), which has relatively high subsidence from overthrusting by the Shillong Plateau (Fig. 1.4; Allison, 1998; Johnson and Nur Alam, 1991).

The GBMD receives the majority of its sediment from the Ganges and Brahmaputra rivers, which transport an estimated ~316-520x10^6 $t{\cdot}yr^{-1}$ and ~540-721x10^6 $t{\cdot}yr^{-1}$, respectively (Islam et al., 1999; Milliman and Syvitski, 1992). Estimates are highly variable due to a lack of data (Milliman and Meade, 1983) and some sources suggest sediment fluxes are instead in the range of 196-480 x10^6 $t{\cdot}yr^{-1}$ in the Ganges River (Allison, 1998; CBJET (China-Bangladesh Joint Expert

Team), 1991; Hossain, 1992) and 387-650x10^6 t·yr^{-1} for the Brahmaputra River (Allison, 1998; FAO (United Nations Food and Agriculture Organization), 1987; Hossain, 1992). The Meghna river carries less sediment (e.g. Wilson and Goodbred Jr., 2015) and estimates are ∼20x10^6 t·yr^{-1} (Allison, 1998; Coleman, 1969). Ultimately, best estimates for the average sediment flux being delivered to the GBMD are one billion tonnes of sediment per year or more (Wilson and Goodbred Jr., 2015). The Ganges River enters the delta to the northwest and drains the Himalayan foreslope (Fig. 1.3A). The Brahmaputra River enters the delta from the northeast, draining the Tibetan backslope, and the Meghna River enters the delta from the east (Fig. 1.3A).

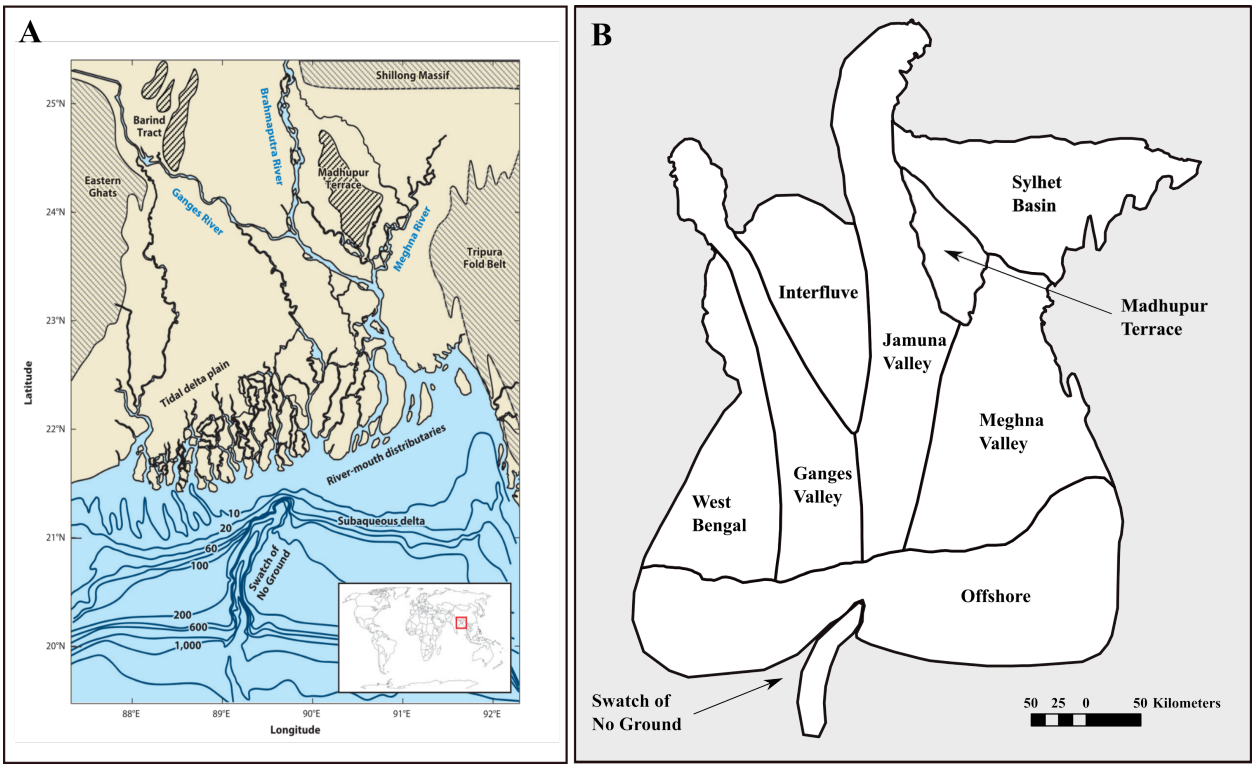

Figure 1.3: Ganges-Brahmaputra-Meghna river delta and morphology. A) Global and regional study site modified from Wilson and Goodbred Jr. (2015). B) Interpreted generalized morphology of the delta. The delta is comprised largely of the river valleys from the Ganges, Jamuna/Brahmaputra, and Meghna rivers. To the north, Sylhet Basin is situated between the Shillong Massif and the Tripura Fold Belt. Madhupur Terrace and the Barind Interfluve sit on top of uplifted Pleistocene topography but contain caps of Holocene sediments.

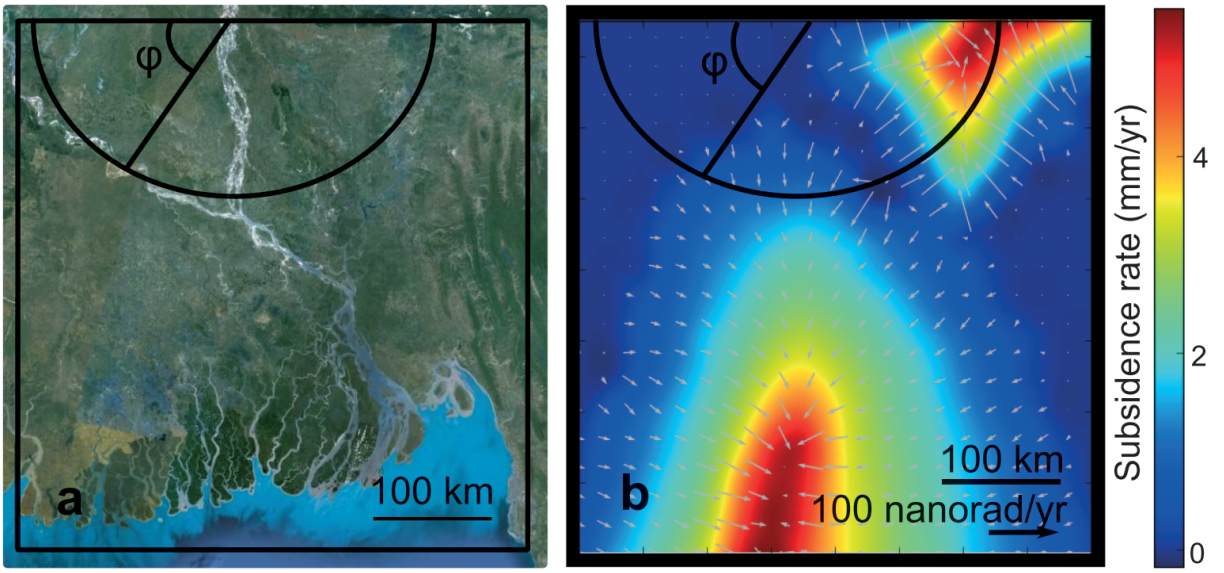

Figure 1.4: Estimates of subsidence rates across the Ganges-Brahmaputra-Meghna river delta (see Reitz et al. (2015) for additional detail and explanation of ψ and subsidence calculation methods). A) Study area showing the delta. B) Subsidence estimates across the delta. Subsidence rates are highest in the low delta and around Sylhet Basin.

Subsidence, tectonics, and geography all influence avulsion frequency and location for the GBMD (Allison, 1998; Reitz et al., 2015; Wilson and Goodbred Jr., 2015). Rivers tend to occupy channels for ∼1000-2000 years prior to avulsion and this behavior is supported by modeling (Reitz et al., 2015), field (Pickering et al., 2014), and laboratory studies (Grimaud et al., 2017). The GBMD has developed through complex lobe-building in response to relatively frequent avulsions along multiple fluvial systems that occupy the delta (Fig. 1.5; e.g. Allison, 1998). Sedimentologic evidence (Allison et al., 2003) suggests that the Ganges River originally occupied a far-western path (now the Hooghly River), allowing the delta to prograde towards the west. Around the same time, the Brahmaputra River likely flowed into and deposited sediment in Sylhet Basin. Both rivers avulsed towards the central delta throughout the late Holocene, becoming confluent and occupying their present positions within the last ∼200 years (Allison et al., 2003).

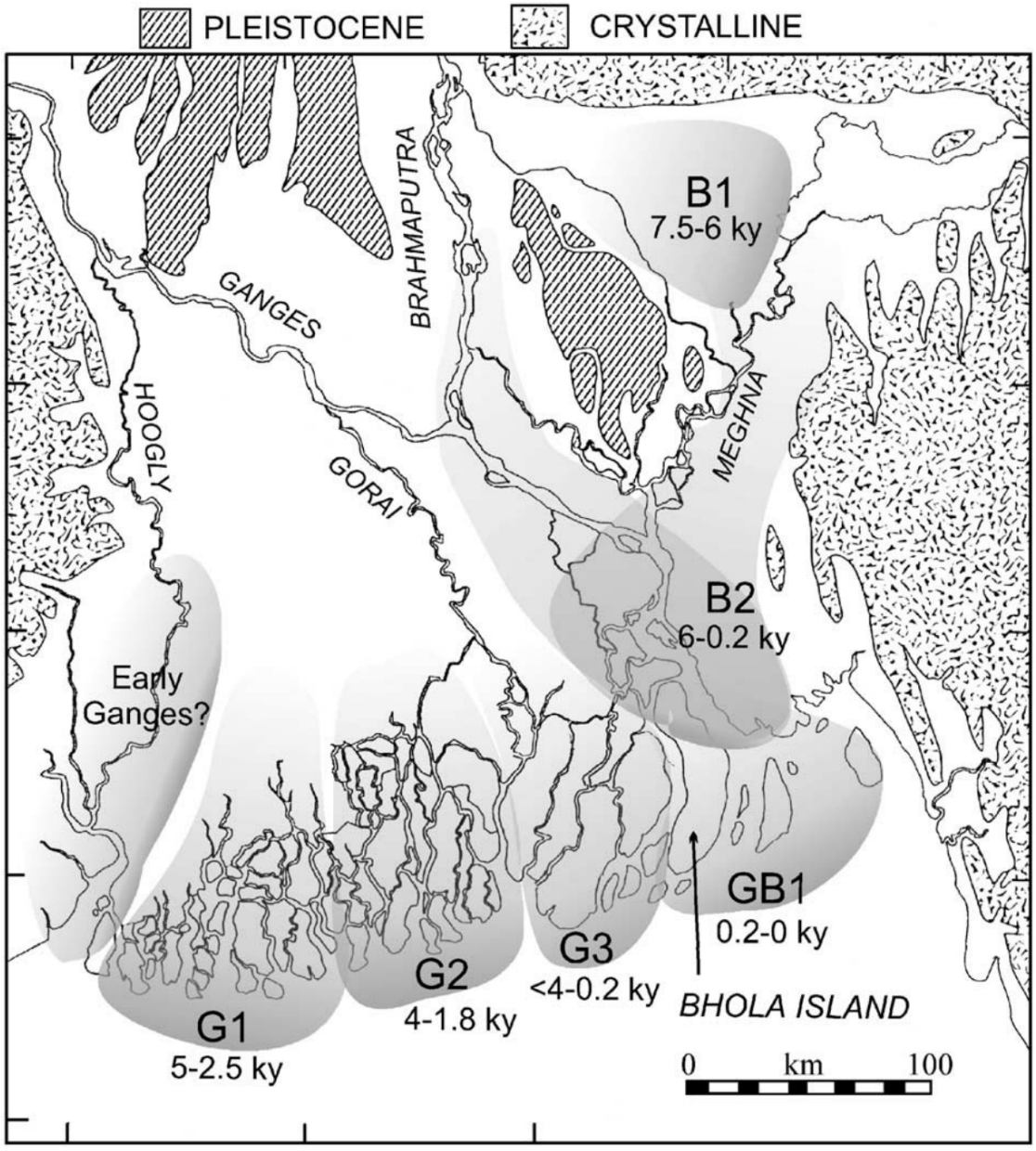

Figure 1.5: Former river pathways and delta lobes for the Ganges-Brahmaputra-Meghna river delta from Allison et al. (2003). Antecedent Pleistocene topography is found in the Barind Interfluve and Madhupur Terrace regions of the delta. During the early Holocene, the Ganges River was likely flowing through the Hooghly River and avulsed east in the late Holocene. The Brahmaputra River flowed through Sylhet Basin during the mid-Holocene, then routed west around Madhupur Terrace to flow through its modern channel. The Brahmaputra and Ganges rivers became confluent $\sim$200 years ago, and the delta is currently prograding along this eastern lobe.

1.3.2 Climate

Bangladesh and India have a highly seasonal climate due to the ISM, which occurs in response to pressure differences between the Tibetan Plateau and Indian Ocean (Rashid et al., 2011). The pressure differences are the result of seasonal winds (Rashid et al., 2011) and ultimately cause a rainy season between May and September and a dry season from October to April. During the rainy season, the GBMD receives 80% of its annual precipitation (e.g. Allison, 1998; Kale et al., 2004; Kumar et al., 2014), >80% of annual fluvial discharge (Coleman, 1969; Goodbred Jr. and Kuehl, 1998; Pate et al., 2009) and 95% of annual fluvial sediment delivery (Pate et al., 2009).

The ISM has been active since the late Miocene (∼8 million years; Kale et al., 2004; Zhisheng et al., 2001) and the strength of the monsoon varies on seasonal and annual to orbital time scales (e.g. Goswami and Mohan, 2001; Hein et al., 2017; Kale et al., 2004; Kale, 2007; Rashid et al., 2011; Zhisheng et al., 2001). The strength of the ISM has varied throughout the Holocene (Fig. 1.6). It was initially strengthened in the early Holocene prior to weakening in the mid-Holocene. Proxy records suggest that the monsoon began to strengthen again during the late Holocene and climate models (although highly uncertain; Goswami and Mohan, 2001; Kumar et al., 2014; Turner and Annamalai, 2012) suggest that this trend may continue into the future, bringing more pronounced wet/dry seasons (e.g. Rahman and Lateh, 2017; Whitehead et al., 2015). As a result, Bangladesh and potentially parts of India could see increased occurrence of dry-season drought and wet-season flooding (Whitehead et al., 2015).

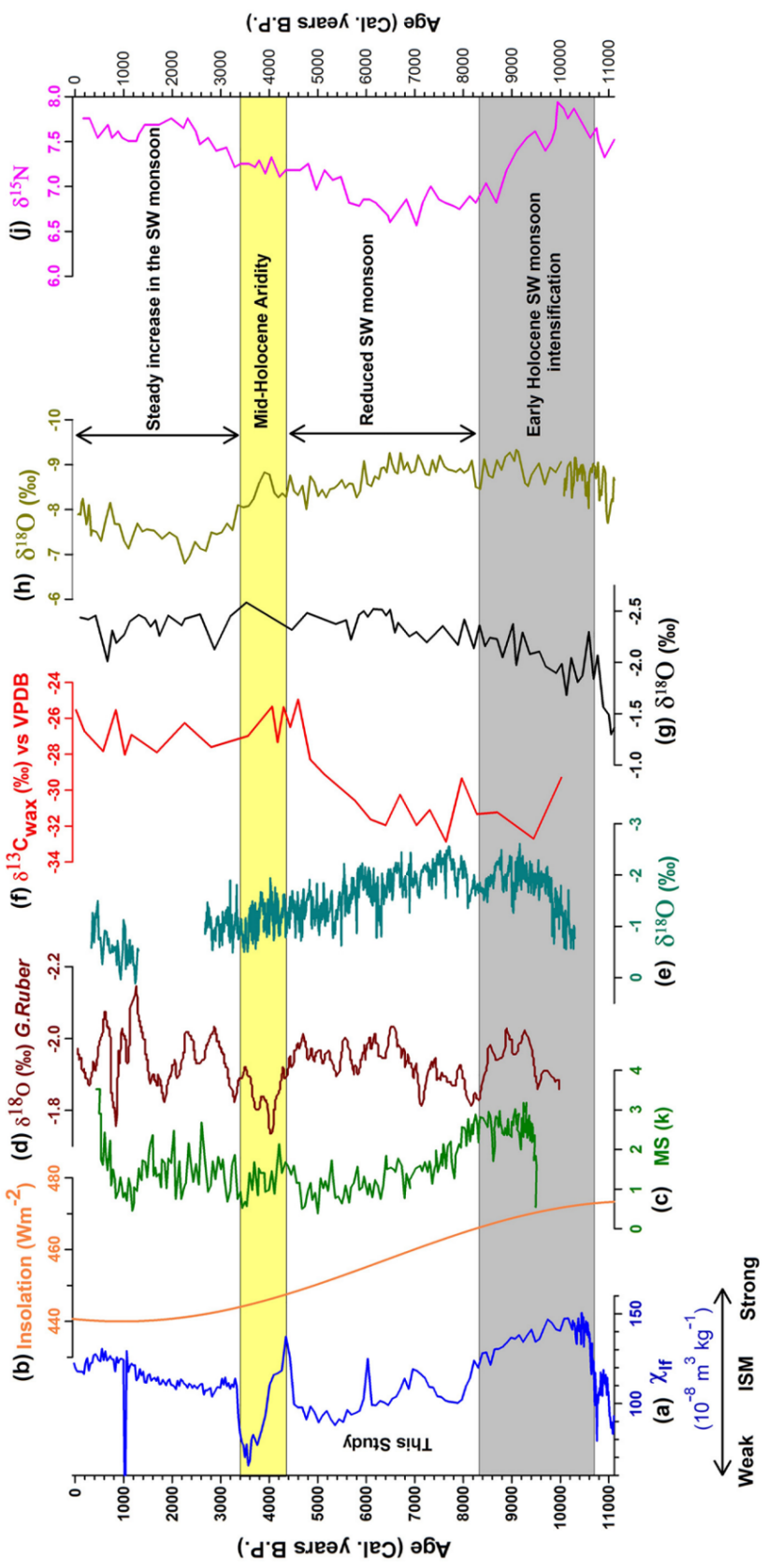

Figure 1.6: Compilation of multiple proxy records showing changes in monsoon strength over the Holocene from Sandeep et al. (2017). These records show a relatively enhanced early-Holocene monsoon, which weakened during the mid-Holocene prior to intensification over the late Holocene and into the present.

Chapter 2

Methods

2.1 Mass-balance framework

Mass-balance approaches to fluvial systems stem from a classic source-to-sink framework, where sediments derived from a source region are transported through the system prior to deposition (Fig. 2.1; Allen, 2017, and the references cited therein). Sediments may experience temporary deposition, transport, and reworking along the source-to-sink pathway. River deltas are one such depocenter, and delta sediments may undergo short-term or permanent storage. The main focus in a mass-balance approach is the sediment load, considered from source-to-sink (Strong et al., 2005), but more complex applications may include effects from subsidence, tectonics, weathering, compaction, etc. (Paola and Voller, 2005). A mass-balance approach to sediment budgets applies a non-dimensional framework that relates the position in the system to the amount of the input sediment load that has been deposited up to that point (Michael et al., 2013; Paola and Martin, 2012; Strong et al., 2005). Not only does this approach simplify analysis of the system in question, but non-dimensionality also facilitates comparison among different systems (Allen, 2017; Michael et al., 2013; Paola and Martin, 2012; Strong et al., 2005).

This research focuses on the Holocene GBMD (Fig. 1.3B). Properties of a mass-balance approach are applied to analysis of the GBMD's Holocene sediment budget through quantification of mass of sediment entering the delta from Himalayan source terrains and being transported offshore of the delta. Sediment dispersal, sequestration, and remobilization on the subaerial and subaqueous parts of the delta are explored as they relate to sediments being transported by the Ganges and Brahmaputra rivers. The stratigraphy, a sequence of $>$90 m of Holocene sediments (sands, silts, clays; Allison et al., 2003; Goodbred Jr. and Kuehl, 2000; Umitsu, 2014, 1993) deposited on top of the underlying Pleistocene topography, is an archive of sediment transport over the last 12,000 years and provides an ideal record through which to examine this research area.

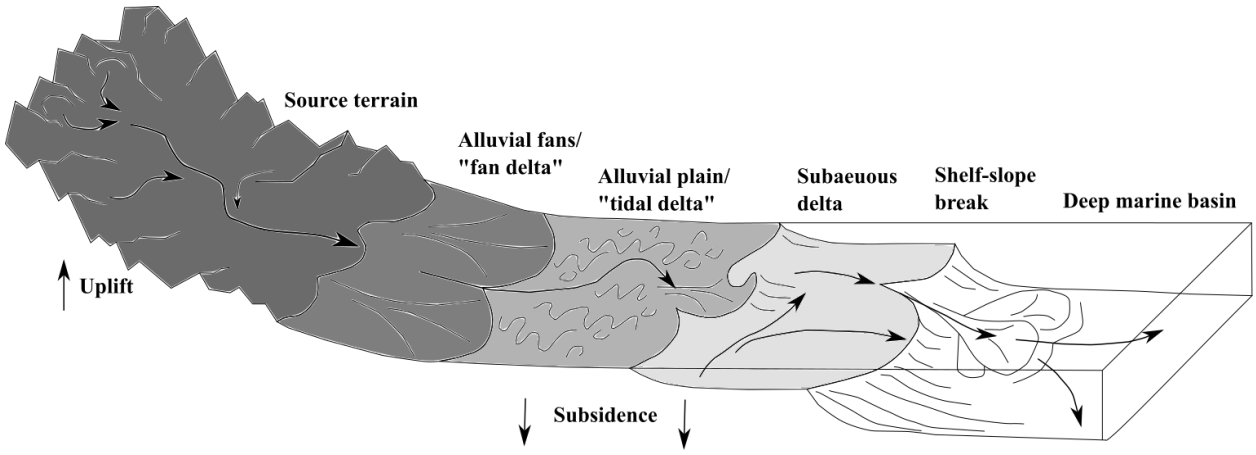

Figure 2.1: A source-to-sink interpretation of a fluvial system modified from Allen (2017). Sediment originates from erosion and weathering in the source terrain and travels down-system to the final sink, the deep-marine basin. In a source-to-sink system, sediment will undergo temporary deposition and remobilization, traveling downstream in a potentially non-linear path. One such area of intermittent storage and remobilization are the alluvial fans/fan delta and alluvial plain/tidal delta. In the Ganges-Brahmaputra-Meghna delta, sediments are transported to the delta by rivers from the Himalayas (source terrain) prior to sediment deposition and reworking in the upper (fan) and lower (tidal) delta. Sediment is transported offshore to the subaqueous delta. Some sediment is lost to the deep sea through the subaqueous canyon, the Swatch of No Ground.

2.2 Field methods

Over 400 boreholes (with a maximum drilling depth of 90 m) were collected in 23 transects across the GBMD during previous field excursions as part of the BanglaPIRE project (Fig. 2.2). Samples were taken every meter with depth and photographed, described according to color, texture, and basic grain size classification, and packaged in the field. More robust analyses of grain size, in addition to bulk geochemical analysis, are performed in the laboratory. Additional drilling campaigns are anticipated for regions with limited data in the central and lower delta. The same drilling and documentation procedures will be followed when collecting the new samples.

2.3 Laboratory analysis and mapping

Samples are analyzed in the lab for bulk geochemistry using a handheld Thermoscientific Niton XL3 Analyzer (XRF), which returns information on bulk composition of both major and trace

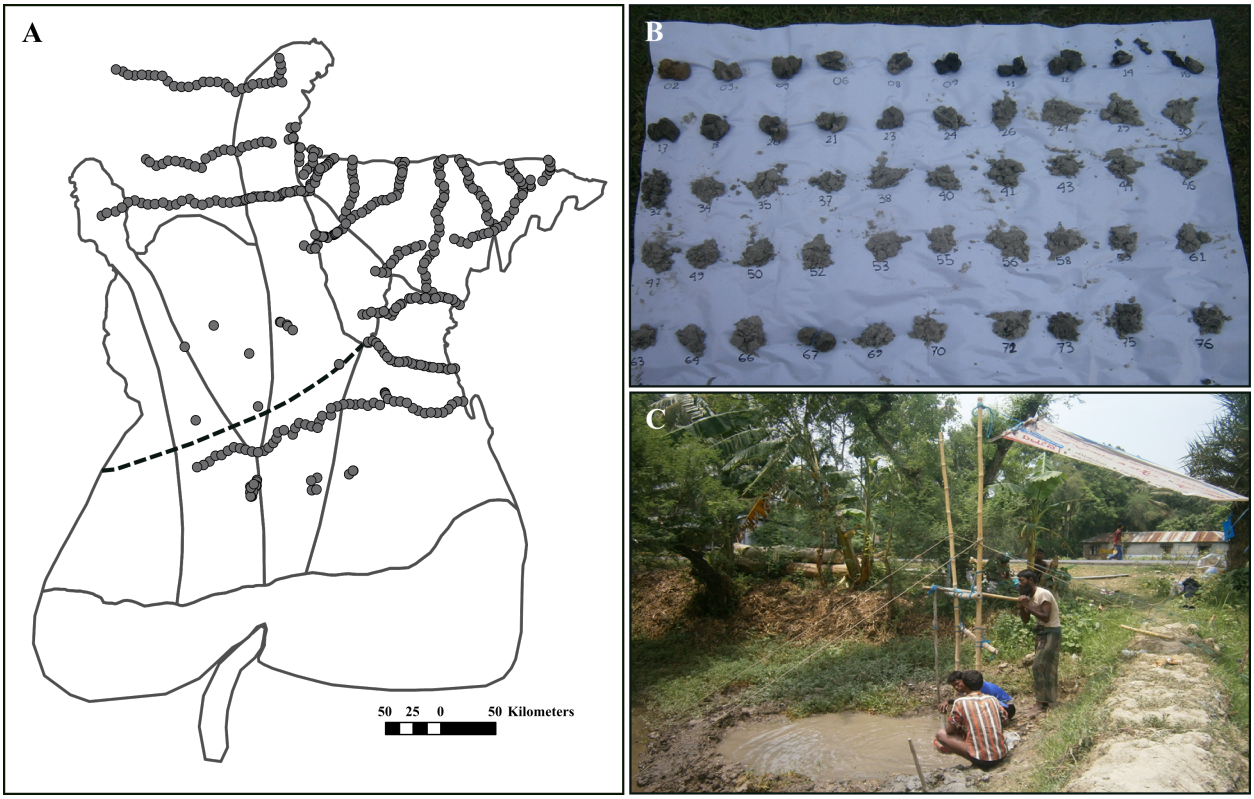

Figure 2.2: Collection of sediment samples from boreholes. A) Over 400 boreholes have been collected on prior field campaigns as part of the NSF-funded BanglaPIRE project. Borehole locations are denoted by the circles. The dashed line represents the slope break between the upper (fan) and lower (tidal) delta. Note that the Ganges Valley and Jamuna Valley physiographic regions are separated into two parts, one above the slope break and one below. For the Meghna region, Sylhet Basin is considered to be representative of the upper Meghna Valley. B) After drilling, samples are photographed, described, and packaged in the field. C) Borehole drilling is facilitated through local partners and collaboration with researchers at Dhaka University.

elements in the sediments. We are predominantly interested in bulk strontium content ([Sr]). Previous work (Goodbred Jr. et al., 2014; Pate, 2008; Pate et al., 2009; Pickering et al., 2014; Singh and France-Lanord, 2002) has shown that Sr concentration is a helpful tracer of river provenance of sediment in the GBMD system, particularly when differentiating between sediments sourced by the Ganges vs. Brahmaputra rivers (Table 2.1) and when examined against data on local variables such as sediment age, geographic location, and weathering history. Low concentrations of strontium likely reflect reworked and weathered Pleistocene materials or sediments deposited by the Meghna river (e.g. Pickering et al., 2014). Values ranging from ∼70-90 ppm are within the

signatures of the Tista River and Shillong region, draining the eastern reaches of the Himalayas (Pate, 2008; Pate et al., 2009; Pickering et al., 2014). Sediments deposited by the Ganges River typically have bulk strontium concentrations ranging from ∼90-110 ppm, although it is difficult to differentiate Ganges materials from mixed-source materials (∼110-140 ppm), as Brahmaputra River sediments have strontium concentrations exceeding ∼140 ppm (Goodbred Jr. et al., 2014; Pate, 2008; Pate et al., 2009; Pickering et al., 2014; Singh and France-Lanord, 2002).

Range (ppm)	**River Provenance**
<70	Meghna River, weathered and reworked Pleistocene materials
70-90	Tista River, Eastern Himalaya, Shillong
90-110	Ganges River
110-140	Mixed source (Likely Ganges and Brahmaputra influence)
>140	Brahmaputra River

Table 2.1: The bulk strontium content of sediment provides information on sediment source terrain and river provenance in the Ganges-Brahmaputra-Meghna river delta system when considered alongside data on geographic location, weathering, and sediment age (Goodbred Jr. et al., 2014; Pate, 2008; Pate et al., 2009; Pickering et al., 2014; Singh and France-Lanord, 2002).

Grain size analysis is also conducted on samples. We target every third depth sample (typically every ∼2-5 m in depth) and also samples at sedimentologic contacts to capture a sufficiently robust understanding of grain-size distributions throughout delta stratigraphy. Samples are sieved through a 1000 μm (0 phi) filter and mixed into a slurry with deionized water prior to analysis with a Malvern Mastersizer 2000 particle size analyzer. Since the beginning of the BanglaPIRE project, over 6,000 of the >15,000 samples have been analyzed for grain size. More than 4,000 of these samples are Holocene-aged and included in this study.

Mapping of the Holocene GBMD was performed with ArcGIS. The Holocene-Pleistocene boundary depth was mapped first by hand using grain size and radiocarbon data from the BanglaPIRE dataset and supplemented with depth data from additional cores and wells (Ahmed et al., 2010; BADC (Bangladesh Agricultural Development Corporation), 1992; DPHE-JICA (Department of Public Health Engineering and Japanese International Cooperation Agency), 2006; Ghosal et al.,

2015; Hait et al., 1996; Hoque et al., 2012; Khan and Islam, 2008; Michels et al., 1998; Palamenghi et al., 2011; Sarkar et al., 2009). Linear kriging was used to create an interpolated surface of the depth of the Pleistocene boundary from these measurements, making predictions about the depth of the Pleistocene surface across the whole delta. Since boreholes are not evenly distributed across the GBMD, we divide the Holocene delta according to the physiography outlined by Figure 1.2B (West Bengal, Ganges Valley, Barind Interfluve, Jamuna Valley, Madhupur Terrace, Sylhet Basin, Meghna Valley, Offshore, Swatch of No Ground). Divisions between physiographic provinces were based on stratigraphic data, surface morphology, and information on antecedent Pleistocene topography. While the division of the delta into physiographic regions (combined with geochemistry) does not necessarily capture all the details related to fluvial source of sediment, it is useful for understanding sediment storage in the regions where samples are limited and stratigraphy is complex.

2.4 Sediment budget calculations

The GBMD's Holocene sediment package includes sediment stored on both the subaerial and subaqueous portions of the delta, but excludes sediment that is funneled through the Swatch of No Ground to deep marine storage. Volumes of stored Holocene sediments are calculated from the interpolated "depth to Pleistocene" surface. To understand the spatial variations in the distribution of sediment storage, the volume of Holocene sediment is calculated for each physiographic province, as well.

Well-constrained estimates of sediment bulk density from previous studies and geo-technical drilling (Kuehl et al., 1997; JICA (Japan International Cooperation Agency), 1976) are used to convert volume estimates to mass fluxes. For sediment deposited in the subaerial delta, bulk density estimates are assigned based on depth to account for the effects of compaction (Table 2.2). A bulk density of 1.2 $g \cdot cm^{-3}$ is used for sediments stored offshore in the subaqueous portion of the delta. Bulk densities are multiplied by the volume of sediment stored in the appropriate depth range or region, summed together, and then divided by the time since deposition to calculate sediment mass

storage rates for the delta.

Radiocarbon ages [from the BanglaPIRE database; (Grall et al., 2018; Pickering et al., 2014)] and subsidence data (e.g. Grall et al., 2018; Reitz et al., 2015; Wilson and Goodbred Jr., 2015) are used to estimate Holocene sea-level changes, in addition to the depositional age of sediments stored within the stratigraphic record (Fig. 2.3). Based on the local sea-level curve for the GBMD (Fig. 2.3), sediments stored between 90 and 30 meters in depth are generally from the early Holocene (12,000-8,000 yrs BP). The upper 30 meters are generally from the mid- to late-Holocene (8,000 yrs BP to present). Rates of sediment deposition in the mid-late Holocene are lower than in the early Holocene, blurring any clear distinctions between depth and age in the upper 30 m of stratigraphy, which is still likely being reworked by the delta's fluvial network. The sediment package is grouped into three time ranges: the early, mid- to late-Holocene, and entire Holocene.

Depth (m) or Region	**Bulk Density ($g \cdot cm^{-3}$)**
0-30	1.5
30-45	1.6
45-60	1.7
60-90	1.8
Offshore	1.2

Table 2.2: Estimates of bulk densities for sediments stored at different depths and for material stored in the offshore (subaqueous) portion of the delta. Values are based on geo-technical drilling and prior offshore research (Kuehl et al., 1997; JICA (Japan International Cooperation Agency), 1976).

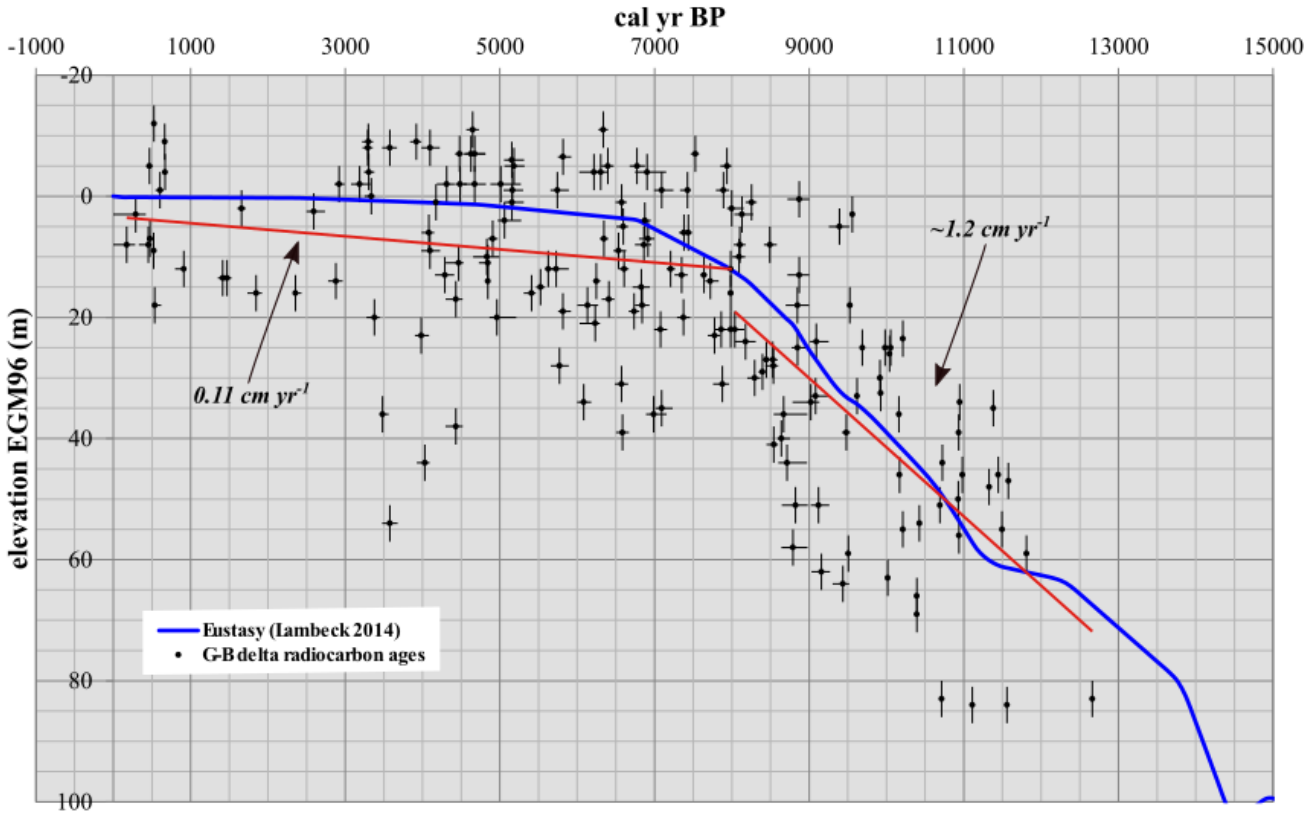

Figure 2.3: Holocene sea-level change for the Ganges-Brahmaputra-Meghna river delta (modified from Goodbred, 2018, pers. comm.). Relative sea-level change is calculated from >170 radiocarbon samples taken from cores shown in Figure 2.2. Eustatic sea-level is shown by the blue line. Radiocarbon dates largely trend with eustacy. The red lines indicate the rate of relative sea-level rise during the early Holocene (12,000 to 8,000 yrs BP) and the late Holocene (8,000 yrs BP to present). Rates of relative sea-level rise were much higher during the early Holocene than in the mid- to late-Holocene.

Chapter 3

Results

3.1 The Holocene sediment package

The Pleistocene surface (Fig. 3.1) exhibits a three-pronged shape and is located deepest in the central delta and along river valleys. There is less Holocene sediment stored towards the perimeter of the delta and also on the uplifted and exposed Pleistocene materials like Madhupur Terrace and the Barind Interfluve (Fig. 1.3). Calculations of the volume of Holocene sediment stored on the delta vary based on physiographic province (Table 3.1). The largest amounts of sediment (on the order of 10^3 km^3 of sediment) are stored in the river valleys. The interpolation shows that a similar volume of sediment is stored offshore in the subaqueous delta. The interfluve and terrace regions store smaller volumes of sediment, suggesting that their uplifted morphology has limited the ability for sediment deposition. To better compare the physiographic regions, we normalized the volumes of Holocene sediment by the area to derive the mean thickness of the Holocene sediment package. On average, the river valleys store $\sim$55-60 m of Holocene sediments. In Sylhet Basin, which stores a relatively small volume of sediment, the thickness of the Holocene sediment package is comparable to that of the offshore sink $\sim$40 m. The interfluves and terraces contain the thinnest Holocene sediment package. However, the Barind Interfluve and West Bengal regions store much more sediment than Madhupur Terrace, where the Holocene package extends only $\sim$5 m in depth, on average.

Radiocarbon analysis on sediment samples collected across the delta helps to place the Holocene sediment sequences in chronological context. Collectively, over 7,630 km^3 of sediment have been stored on the GBMD over the Holocene (Table 3.2). Based on the sea level curve and radiocarbon analysis, the sediments are partitioned between early Holocene (12,000-8,000 yrs BP) and mid-late Holocene (8,000 yrs BP-present) based on depth (Fig. 2.3). Since sediments stored at depths $<$30 m are considered mid-late Holocene, the interfluves and terrace regions fall completely

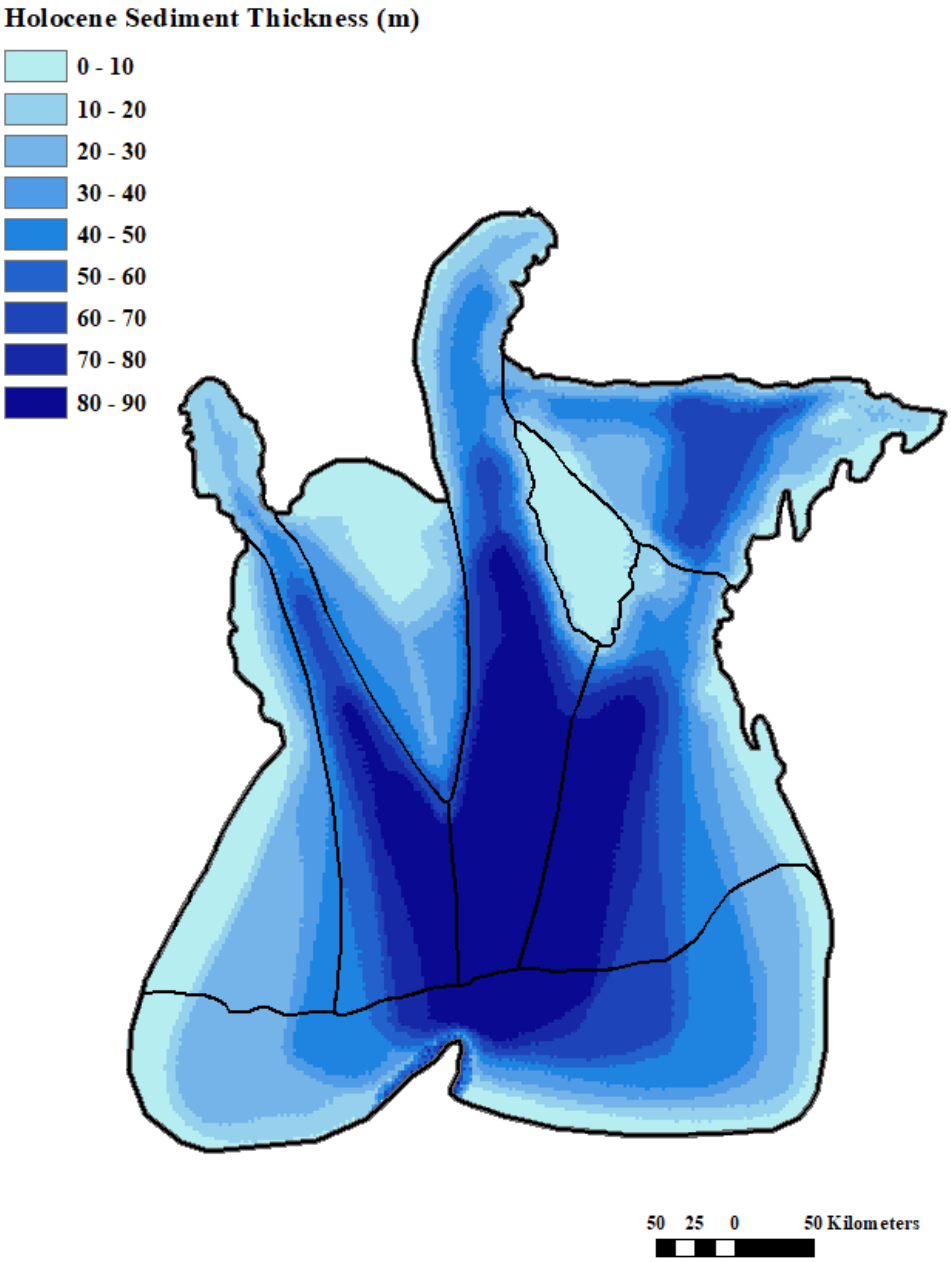

Figure 3.1: Interpolated surface showing the thickness of the Holocene sediment package. This surface was created in ArcGIS using linear kriging. The Pleistocene surface is deepest in the central Ganges-Brahmaputra-Meghna river delta and along the river valleys, notably the Ganges and Jamuna valleys. Holocene sediments are thinner on the edges of the delta and in regions like the raised Pleistocene Madhupur Terrace, which is covered by $<$10 m of Holocene sediments.

within the last 8,000 years of the Holocene Epoch (Table 3.1). The basins and river valleys, however, contain relatively thicker stratigraphic sequences and were storing sediment during the early Holocene. When the sediments are partitioned accordingly, 3,240 km^3 of sediment were stored during the early Holocene and 4,390 km^3 have been stored during the mid-late Holocene. These storage amounts relate to sediment discharges that are on the order of $1.00x10^9$ $t \cdot yr^{-1}$ over the entire Holocene, which is effectively the flux of sediment being transported to the delta by the Ganges and Brahmaputra rivers today. This calculated storage rate suggests that with similar mass inputs, sediment sequestration was occurring at high rates with near complete storage over the Holocene. However, when storage rates are calculated for the early and mid-late Holocene time periods separately, storage rates are higher during the early Holocene than during the mid-late Holocene by nearly 1.5x. In the early Holocene, sediment storage was occurring at a rate of $1.37x10^9$ $t \cdot yr^{-1}$ compared to a rate of $0.82x10^9$ $t \cdot yr^{-1}$ in the mid-late Holocene. A storage rate of $1.37x10^9$ $t \cdot yr^{-1}$ exceeds estimates of modern fluvial sediment loads, indicating that additional sources of sediment must have been present during the early Holocene. These storage rate calculations also provide further support for high sediment trapping efficiency on the GBMD.

Physiographic Region	Area (km^2)	Volume (km^3)	Mean thickness (m)
River Valleys			
Jamuna Valley	$2.70x10^4$	$1.70x10^3$	62.9
Ganges Valley	$1.80x10^4$	$1.10x10^3$	61.1
Meghna Valley	$2.71x10^4$	$1.51x10^3$	55.9
Interfluves and Terraces			
Barind Interfluve	$1.42x10^4$	$0.35x10^3$	24.4
Madhupur Terrace	$0.47x10^4$	$0.02x10^3$	4.3
West Bengal	$1.69x10^4$	$0.39x10^3$	22.9
Basins			
Sylhet Basin	$1.91x10^4$	$0.71x10^3$	37.0
Offshore	$4.16x10^4$	$1.62x10^3$	38.8

Table 3.1: Volume estimates for the Ganges-Brahmaputra-Meghna river delta's physiographic regions (Figs. 1.2B, 3.1). Volumes were calculated from the interpolated surface of Holocene Sediment thickness (Fig. 3.1) in ArcGIS. The majority of Holocene sediments are stored in the river valleys and in the offshore basin. The Barind Interfluve, Sylhet Basin, and West Bengal regions also store several hundred cubic kilometers of Holocene sediment. The volume of the sediment package is normalized to the area of each region to calculate a sediment thickness.

Time (yrs BP)	Volume (km^3)	Storage ($t \cdot yr^{-1}$)
12,000 to present	$7.63x10^3$	$1.00x10^9$
8,000 to present	$4.39x10^3$	$0.82x10^9$
12,000 to 8,000	$3.24x10^3$	$1.37x10^9$

Table 3.2: Volume estimates for the Ganges-Brahmaputra-Meghna river delta. Volumes were calculated using ArcGIS from the interpolated surface of Holocene sediment thickness (Fig. 3.1). Sediment storage rates were then calculated for the volumes based on the estimated sediment bulk densities shown in Table 2.2 and time since deposition.

3.2 Grain size

The grain-size distribution of Holocene sediments varies across the delta and also within each physiographic region (Table 3.3). When grain-size distributions are examined collectively, the whole delta is roughly 30% mud-sized sediments. Delta sands are mostly fine and medium grained ($\sim$50%). Similar calculations applied to each physiographic region suggest that sediments stored in the Jamuna are coarser than elsewhere in the delta, with only 18.6% mud-sized sediments, $>$30% medium sand, and $\sim$12% coarse sands. Sylhet Basin stores $\sim$40% mud-sized sediments but also contains nearly 40% fine and medium sands. The sediments stored in Madhupur Terrace and the Barind Interfluve are muddy (46% and 32% mud, respectively), but these regions also contain $>$35% and $>$40% fine to medium sands, respectively.

Grain-size distributions differ above (fan delta; Table 3.4) and below (tidal delta; Table 3.5) the topographic break on the GBMD. Sylhet Basin represents the upper Meghna Valley sediments. When the entire upper delta is considered collectively, there are higher percentages of mud and also medium and coarse sand compared to the lower delta. The lower delta has higher percentages of very fine and fine sand, but half as much coarse sand as the upper delta. Partitioning the upper delta into the physiographic regions shows that Sylhet Basin may be partially responsible for the high mud percentages, as it contains $>$40% mud, 12% very fine sand, 19.1% fine sand, 20.2% medium sand, and 8.1% coarse sand. Sylhet Basin has more than 2x as much mud as each of the other two upper river valleys. When the upper delta is considered without Sylhet Basin, the grain-size distribution more closely resembles that of the upper river valley sediments with $\sim$15% mud-sized sediments and $\sim$60% fine to medium sands. The Upper Jamuna Valley contains only 11.4% mud, 6.1% very fine sand, and $\sim$26% fine sand, but contains the highest amounts of medium (39.3%) and coarse sand (17.5%) on the upper delta plain. The upper Ganges Valley is slightly more fine-grained than the Jamuna river, with $>$16% mud, $\sim$8% very fine sand, 28.4% fine sand, 33.4% medium sand, and $\sim$14% coarse sand.

In the tidal portion of the delta plain, the river valley sediments are generally more fine-grained than those stored up-system. In addition, each portion of the lower delta appears to have rela-

tively similar grain-size distributions. The lower delta and lower river valleys are ∼26% mud, 13-16% very fine sand, ∼30% fine sand, ∼22% medium sand, and ∼6% coarse sand. Overall, the percentage of fine sand remains relatively consistent from the fan to the tidal delta, and the most pronounced changes occur with the percentages of mud-sized, very fine, and coarse sediments.

Region	**% Clay** (<3.9 μm)	**% Silt** (3.9-62.5 μm)	**% Very Fine Sand** (62.5-125 μm)	**% Fine Sand** (125-250 μm)	**% Medium Sand** (250-500 μm)	**% Coarse Sand** (500-1000 μm)
Whole delta	3.4	26.3	12.5	24.8	24.3	8.6
River Valleys						
Jamuna Valley	1.6	17.0	10.8	27.4	31.1	12.1
Ganges Valley	2.6	22.7	12.6	29.7	24.9	7.5
Meghna Valley	2.1	23.5	16.1	30.2	22.7	5.4
Interfluves and Terraces						
Barind Interfluve	9.2	23.1	17.2	23.6	17.6	9.3
Madhupur Terrace	5.7	40.5	8.7	15.2	21.8	8.1
Basins						
Sylhet Basin	5.3	35.3	12.0	19.1	20.2	8.1

Table 3.3: Grain-size distribution of the Holocene sediment package, partitioned by physiographic region. The BanglaPIRE database does not contain samples for sediments stored in West Bengal or Offshore and these regions are omitted.

Region	**% Clay** (<3.9 μm)	**%Silt** (3.9-62.5 μm)	**% Very Fine Sand** (62.5-125 μm)	**% Fine Sand** (125-250 μm)	**% Medium Sand** (250-500 μm)	**% Coarse Sand** (500-1000 μm)
Upper Jamuna Valley	0.9	10.9	6.2	25.3	39.0	17.7
Upper Ganges Valley	1.4	15.1	7.8	28.4	33.4	13.9
Sylhet Basin *(Upper Meghna Valley)*	5.3	35.3	12.0	19.1	20.2	8.1
Total Upper Delta *(with Sylhet Basin)*	3.9	28.0	10.4	21.1	25.7	10.9
Total Upper Delta *(without Sylhet Basin)*	1.4	14.0	7.4	24.9	36.1	16.2

Table 3.4: Grain-size distribution of the Holocene sediment package stored in the upper, fan delta. Sediments are grouped by physiographic region and only whole-delta and river valley sediments are included. Due to the high mud content of Sylhet Basin sediments, the upper delta total is calculated both with and without Sylhet Basin sediments included.

Region	**% Clay** (<3.9 μm)	**% Silt** (3.9-62.5 μm)	**% Very Fine Sand** (62.5-125 μm)	**% Fine Sand** (125-250 μm)	**% Medium Sand** (250-500 μm)	**% Coarse Sand** (500-1000 μm)
Lower Jamuna Valley	2.3	24.1	16.2	29.8	21.9	5.7
Lower Ganges Valley	2.8	23.9	13.3	29.9	23.6	6.5
Lower Meghna Valley	2.1	23.5	16.1	30.2	22.7	5.4
Total Lower Delta	2.6	24.0	15.3	29.8	22.5	5.8

Table 3.5: Grain-size distribution of the Holocene sediment package stored in the lower, tidal delta. Sediments are grouped by physiographic region and only whole-delta and river valley sediments are included.

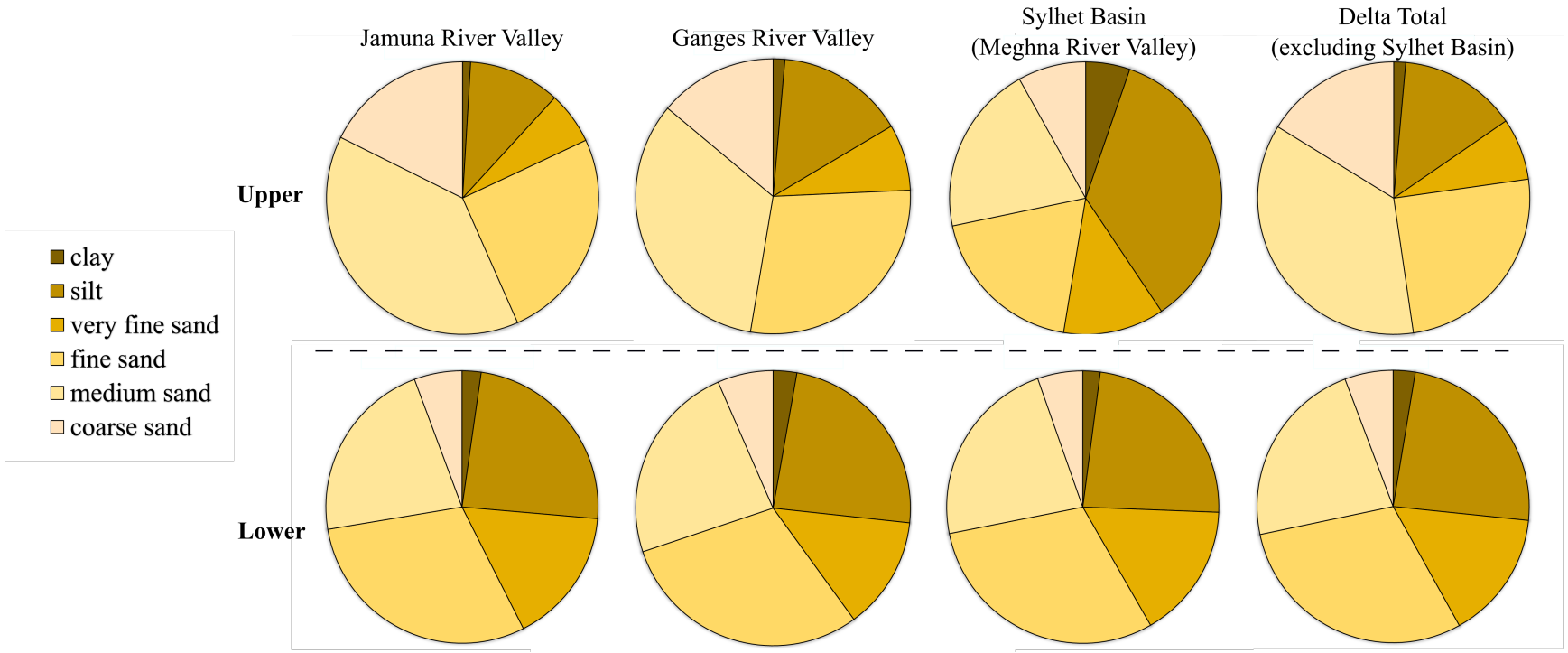

Figure 3.2: Comparison of grain-size distributions between the upper and lower Holocene delta and river valleys. The upper delta is characterized by a larger percentage of medium to coarse sands, while sediment stored in the lower delta generally contains more mud and very fine to fine sands.

Region	[Sr] Range (ppm)	Average [Sr] (ppm)	Number of Samples
Ganges River system			
Upper Ganges Valley	63-120	85	17
Lower Ganges Valley	27-141	95	360
Jamuna River system			
Upper Jamuna Valley	35-212	139	409
Lower Jamuna Valley	53-183	129	489
Sylhet Basin & Meghna River system			
Sylhet Basin (Upper Meghna Valley)	8-210	110	1615
Lower Meghna Valley	29-209	130	571

Table 3.6: Range in strontium concentrations, in addition to average strontium concentration, for sediments stored in the Ganges, Jamuna, and Meghna river valleys.

3.3 Bulk strontium and river provenance

3.3.1 Ganges River physiography and sediment provenance

In the upper Ganges Valley, bulk strontium content of sediments ranges from low concentrations $\sim$60 ppm, characteristic of reworked Pleistocene materials, to $\sim$120 ppm, well into the expected range for sediments deposited by the Ganges River. Although the sample size is small (n=17), sediments deposited at depths greater than 10 m on average have lower strontium concentrations ranging from 63 ppm to 92 ppm. The highest strontium concentrations occur in surface sediments, although surface sediments exhibit some variability in strontium values ranging from 76 ppm to 120 ppm. Seven samples are within the expected range for Ganges-derived sediments. The average strontium concentration for all upper Ganges samples is $\sim$85 ppm, suggesting influence of the Tista River and Eastern Himalayan/Shillong-sourced sediments.

In the lower Ganges Valley, strontium concentrations of sediments range from low values of $<$30 ppm to high values of 141 ppm. The average strontium concentration for sediments stored in the lower Ganges Valley is within the expected range for Ganges sediments at 95 ppm. Two-thirds of lower Ganges sediments are within the expected range for the sediment deposited by the Ganges

River (>90 ppm). There is no apparent trend between depth and strontium, but on average, sediments within 20 m of the surface have lower strontium values. The low strontium concentration of surface sediments may potentially indicate some Meghna influence in the lower Ganges plain or weathering and reworking of Pleistocene materials. There is evidence for some input from Eastern Himalayan sources as well.

3.3.2 Jamuna/Brahmaputra River physiography and sediment provenance

Strontium concentrations in upper Jamuna sediments reach values typical of Brahmaputra-sourced sediments, with a maximum concentration of 212 ppm at 12 m depth in a sample taken just upstream of the confluence between the modern Ganges and Brahmaputra rivers. Only 59% of the sediments in the upper Jamuna Valley contain a clear Brahmaputra signature. Lower strontium samples found in the upper Jamuna Valley are likely locally sourced Shillong or Tista sediments.

The lower Jamuna Valley sediment package exhibits similar trends in the strontium concentration to that of the upper Jamuna Valley. Values range from 53 ppm to 183 ppm, with an average concentration of $\sim$129 ppm. Sediments containing a Brahmaputra signature (>140 ppm) occur at an average depth of 30 m (n=191). In the mid-late Holocene, the Ganges River shifted paths towards the east to flow through the central and lower Jamuna Valley and deposit sediment (Allison et al., 2003). Therefore, the shallow Jamuna Valley sediments may be sourced by the Ganges River.

3.3.3 Meghna River physiography and sediment provenance

The Meghna River Valley is a more complicated archive of river provenance than the Jamuna and Ganges river valleys. The upper portion of the valley is the large depocenter, Sylhet Basin, which is tectonically active and an episodic river path and depocenter for the Brahmaputra River (Pickering et al., 2014; Sincavage et al., 2018). One-third of the sediments stored in Sylhet Basin have low strontium concentrations indicative of reworked and weathered Pleistocene materials or inputs from Shillong.

The lower portion of the Meghna River Valley has a similar range in sediment strontium concentrations as the upper Meghna Valley, but the average is $\sim$130 ppm. Half of the sediments stored in the lower Meghna River Valley are derived from a Ganges source, while $\sim$40% of the sediments are derived from the Brahmaputra River.

Chapter 4

Discussion

4.1 Sediment storage

The volume and spatial distribution of Holocene sediments show sediment is dominantly stored within the river valleys. This is consistent with knowledge on lobe-building processes and delta development because sediment delivery by rivers is concentrated near the river channels. Bulk strontium content provides support for river valley storage, as the strontium signatures of sediments largely reflect their depositional physiographic region (Table 3.6). The relatively thin Holocene sediment packages in uplifted Pleistocene terrains such as the Barind Interfluve, Madhupur Terrace, and West Bengal regions suggest that antecedent Pleistocene topography may influence sediment storage. The hummocky, incised shape of the Pleistocene surface (Fig. 3.1) influences the space available for sediment storage, with more space in valleys and basins than uplifted terrains. In addition, Pleistocene topography also plays a role in sediment storage through its controls on river path and behavior (e.g. Pickering et al., 2014). The Brahmaputra River switched course from flowing through Sylhet Basin, where it was experiencing aggradation due to mobility constraints from Pleistocene topography (Pickering et al., 2014), to flowing around the western edge of Madhupur Terrace $\sim$6,000 years ago (Allison et al., 2003). This river avulsion to its modern channel allowed for sediment delivery and storage in the vicinity of the modern Brahmaputra-Jamuna River Valley, in addition to facilitating accumulation of mid-late aged Holocene floodplain (*i.e.* fine-grained) sediments in Sylhet Basin.

Subsidence and relative sea-level rise are also important factors in creating accommodation for sediment storage on the GBMD. Subsidence rates are still poorly understood for the GBMD and vary across the delta. High rates of subsidence in Sylhet Basin and in the tidal portion of the delta (Fig. 1.4) provide space for sediment storage, which is reflected in the thickness of the Holocene sediment package (Fig. 3.1). The Holocene package is deepest in the Sylhet Basin area and in

the lower river valleys. Radiocarbon dates and the regional Holocene sea-level curve (Fig. 2.3) also provide evidence for rapid sediment deposition during rates of high relative sea-level rise and increased accommodation. For example, during the early Holocene (12,000-$\sim$8,000 yrs BP), sea level rose at 1.2 cm$\cdot$yr^{-1} and nearly 60 m of sediment was deposited and stored on the delta. However, sediment deposition slowed with sea level and only $\sim$30 m of sediment have been deposited during the last 8,000 years.

4.2 Sediment flux and transport

Despite high rates of sea-level rise and subsidence in the early Holocene, sediment storage estimates suggest that early-Holocene storage was occurring at a rate nearly 1.5x greater than the long-term Holocene average. In addition, estimated storage rates over the Holocene suggest that on average, one billion tonnes of sediment were stored each year. Assuming similar mass inputs to the present, the delta would be experiencing nearly complete storage efficiency. This would indicate that relatively little sediment is lost from the subaerial and subaqueous portions of the delta to the Swatch of No Ground. Storage has been occurring at a slower rate across the delta for the past 8,000 years. This complements earlier studies that suggested a doubling of the early Holocene sediment flux compared to the long-term average (e.g. Goodbred Jr. and Kuehl, 2000). These earlier studies suggest that monsoon strength may play a role in altering the sediment flux, and hence storage rate, on the delta. The results of this research suggest that rates of early Holocene sediment storage exceeded modern fluvial mass inputs. Multiple proxy records document fluctuations in ISM strength over the Holocene, with a relatively strong monsoon coinciding with this period of increased sediment storage in the early Holocene (Sandeep et al., 2017). In addition, decreased rates of sediment storage over the last 8,000 years correspond to a weakening of the monsoon during the mid-late Holocene (Sandeep et al., 2017, and the references cited therein). While the strong early-Holocene monsoon may have provided a mechanism to mobilize sediments stored in the source terrains (e.g. Goodbred Jr. and Kuehl, 2000), little research has been performed to understand the source of sediment.

4.3 Future directions

This work is the foundation for continued exploration into GBMD development, growth, and change over the Holocene. Future study will use the BanglaPIRE database to investigate the relationship between monsoon strength and changing sediment supply, with a specific focus on the source of sediment for high early Holocene fluxes to the delta. Future work will expand this mass-balance framework to address downstream fining on the delta, with particular interest into the mechanisms driving observed fining patterns in surface sediments and the stratigraphic record (bedload mass extraction vs. backwater hydrodynamic effects). This work may potentially provide insights into quantifying stratigraphic preservation and bias in the GBMD delta stratigraphy.

Chapter 5

Conclusions

Holocene development of the GBMD was heavily influenced by interactions between climate, sediment supply, and sea-level changes. Correspondence between increased monsoon strength, high rates of sediment storage, and high rates of relative sea-level rise in the early Holocene suggests increased precipitation may have mobilized sediments stored in source terrains and increased accommodation from high sea-level rise may have led to significant, efficient sediment storage on the delta. Grain size and stratigraphic analysis suggest that early-Holocene storage rates exceeded Holocene-averaged rates by nearly 1.5x. During the last 8,000 years, rates have fallen to 80% of average. The spatial distribution of sediment storage appears to be highly influenced by antecedent Pleistocene topography, which ultimately influences the amount of space available to deposit and store sediment over the Holocene. The raised Pleistocene terrains of the Barind Interfluve and Madhupur Terrace store very thin layers of Holocene sediments, while the river valleys contain the majority of Holocene sediments. Bulk geochemical analysis suggests some reworking on Pleistocene materials in the river valleys, but ultimately show that deep Holocene material in the central delta is derived from a Ganges source, while Brahmaputra signatures are introduced in the central delta into the upper stratigraphy.

This research suggests that the delta was able to transport and store large volumes of sediment during a strong monsoon and with high rates of sea-level rise, an environmental scenario not unlike recent and projected rates of sea-level rise due to anthropogenic climate change. It is predicted that many deltas may experience partial drowning if sediment supply is insufficient to keep pace with sea-level rise and subsidence. Scientists predict that the monsoon will continue to strengthen. The early Holocene may be an analog for expected changes to the GBMD system, indicating that an increase in the sediment supply to more than one billion tonnes per year may improve delta resiliency.

REFERENCES

Ahmed, A. U. and Alam, M. (1999). *Development of Climate Change Scenarios with General Circulation Models*, pages 13–20. Springer Netherlands, Dordrecht.

Ahmed, M., Islam, S., Rahman, M., Haque, M., and Islam, M. (2010). Heavy Metals in Water , Sediment and Some Fishes of Buriganga River, Bangladesh. *International Journal of Environmental Research*, 4(2):321–332.

Allen, P. A. (2017). *Sediment Routing Systems*. Cambridge University Press, Cambridge.

Allison, M., Khan, S., Goodbred Jr., S., and Kuehl, S. (2003). Stratigraphic evolution of the late Holocene Ganges–Brahmaputra lower delta plain. *Sedimentary Geology*, 155:317–342.

Allison, M. A. (1998). Geologic Framework and Environmental Status of the Ganges-Brahmaputra Delta. *Journal of Coastal Research*, 14(3):826–836.

BADC (Bangladesh Agricultural Development Corporation) (1992). Deep Tubewell II Project: Final Reports.

Blum, M. D. and Roberts, H. H. (2009). Drowning of the Mississippi Delta due to insufficient sediment supply and global sea-level rise. *Nature Geoscience*, 2(7):488–491.

CBJET (China-Bangladesh Joint Expert Team) (1991). Study Report on Flood Control and River Training Project on the Brahmaputra River in Bangladesh. Vol. 1. Analysis of Hydrology and River Morphology of the Brahmaputra River. Technical report, Dhaka, Bangladesh.

Coleman, J. M. (1969). Brahmaputra river: Channel processes and sedimentation. *Sedimentary Geology*, 3(2):129–239.

Day, J. W., Boesch, D. F., Clairain, E. J., Kemp, G. P., Laska, S. B., Mitsch, W. J., Orth, K., Mashriqui, H., Reed, D. J., Shabman, L., Simenstad, C. A., Streever, B. J., Twilley, R. R.,

Watson, C. C., Wells, J. T., and Whigham, D. F. (2007). Restoration of the Mississippi Delta: Lessons from Hurricanes Katrina and Rita. *Science*, 315(5819):1679–1684.

DPHE-JICA (Department of Public Health Engineering and Japanese International Cooperation Agency) (2006). Development of deep aquifer database and preliminary deep aquifer map. Final Report. Technical report.

Dutch Water Sector (2012). Dutch consortium granted contract to assist Vietnamese government in long term Mekong Delta plan.

ESA Earth Online (2015). Mississippi River Delta, USA.

FAO (United Nations Food and Agriculture Organization) (1987). Floods and Storms: Master Plan Organization, Mininistry of Irrigation, Water Development and Flood Control, Bangladesh. Technical report, MPO-UNDP-IBRD Technical Report No. 11.

Galloway, W. E. (1975). Process framework for describing the morphologic and stratigraphic evolution of deltaic depositional systems. In Broussard, M. L., editor, *Deltas: models for exploration*, pages 87–98. Houston Geological Society.

Gersonius, B., Rijke, J., Ashley, R., Bloemen, P., Kelder, E., and Zevenbergen, C. (2016). Adaptive Delta Management for flood risk and resilience in Dordrecht, The Netherlands. *Natural Hazards*, 82(2):201–216.

Ghosal, U., Sikdar, P., and McArthur, J. (2015). Palaeosol Control of Arsenic Pollution: The Bengal Basin in West Bengal, India. *Groundwater*, 53(4):588–599.

Giosan, L., Syvitski, J., Constantinescu, S., and Day, J. (2014). Protect the world's deltas. *Nature*, 516(7529):31–33.

Goodbred Jr., S. L. and Kuehl, S. A. (1998). Floodplain processes in the Bengal Basin and the storage of Ganges-Brahmaputra river sediment: An accretion study using 137Cs and 210Pb geochronology. *Sedimentary Geology*, 121(3-4):239–258.

Goodbred Jr., S. L. and Kuehl, S. A. (1999). Holocene and modern sediment budgets for the Ganges-Brahmaputra river system: Evidence for highstand dispersal to flood-plain, shelf, and deep-sea depocenters. *Geology*, 27(6):559–562.

Goodbred Jr., S. L. and Kuehl, S. A. (2000). Enormous Ganges-Brahmaputra sediment discharge during strengthened early Holocene monsoon. *Geology*, 28(12):1083–1086.

Goodbred Jr., S. L., Paolo, P. M., Ullah, M. S., Pate, R. D., Khan, S. R., Kuehl, S. A., Singh, S. K., and Rahaman, W. (2014). Piecing together the Ganges-Brahmaputra-Meghna river delta: Use of sediment provenance to reconstruct the history and interaction of multiple fluvial systems during Holocene delta evolution. *Bulletin of the Geological Society of America*, 126(11-12):1495–1510.

Goswami, B. N. and Mohan, R. S. A. (2001). Intraseasonal Oscillations and Interannual Variability of the Indian Summer Monsoon. *Journal of Climate*, 14(6):1180–1198.

Grall, C., Steckler, M. S., Pickering, J. L., Goodbred, S., Sincavage, R., Paola, C., Akhter, S. H., and Spiess, V. (2018). A base-level stratigraphic approach to determining Holocene subsidence of the Ganges–Meghna–Brahmaputra Delta plain. *Earth and Planetary Science Letters*, 499:23–36.

Grimaud, J.-L., Paola, C., and Ellis, C. (2017). Competition between uplift and transverse sedimentation in an experimental delta. *Journal of Geophysical Research: Earth Surface*, 122(7):1339–1354.

Hait, A., Das, H., Ghosh, S., Ray, A., Saha, A., and Chanda, S. (1996). New dates of Pleisto-Holocene subcrop samples from South Bengal, India. *Indian Journal of Earth Science*, 23:79–82.

Hein, C. J., Galy, V., Galy, A., France-Lanord, C., Kudrass, H., and Schwenk, T. (2017). Post-glacial climate forcing of surface processes in the Ganges–Brahmaputra river basin and implications for carbon sequestration. *Earth and Planetary Science Letters*, 478:89–101.

Hoque, M. A., McArthur, J. M., and Sikdar, P. K. (2012). The palaeosol model of arsenic pollution of groundwater tested along a 32km traverse across West Bengal, India. *Science of the Total Environment*, 431:157–165.

Hossain, M. M. (1992). Total Sediment Load in the Lower Ganges and Jamuna. Technical report, Bangladesh University of Engineering and Technology International Report.

Islam, M. R., Begum, S. F., Yamaguchi, Y., and Ogawa, K. (1999). The Ganges and Brahmaputra rivers in Bangladesh: basin denudation and sedimentation. *Hydrological Processes*, 13(17):2907–2923.

JICA (Japan International Cooperation Agency) (1976). Vol. 6: Geology and Stone Material, Part 1: Geology. Technical report, Japan International Cooperation Agency, Tokyo, Japan.

Johnson, S. Y. and Nur Alam, A. M. (1991). Sedimentation and tectonics of the Sylhet trough, Bangladesh. *The Geological Society of America Bulletin*, 103(11):1513.

Kale, V. S. (2007). Fluvio-sedimentary response of the monsoon-fed Indian rivers to Late Pleistocene-Holocene changes in monsoon strength: reconstruction based on existing 14C dates. *Quaternary Science Reviews*, 26(11-12):1610–1620.

Kale, V. S., Gupta, A., and Singhvi, A. K. (2004). Late Pleistocene-Holocene Palaeohydrology of Monsoon Asia. *Journal Geological Society of India*, 64(October):403–417.

Karim, M. F. and Mimura, N. (2008). Impacts of climate change and sea-level rise on cyclonic storm surge floods in Bangladesh. *Global Environmental Change*, 18(3):490–500.

Khan, S. R. and Islam, B. (2008). Holocene stratigraphy of the lower Ganges-Brahmaputra river delta in Bangladesh. *Frontiers of Earth Science in China*, 2(4):393–399.

Kuehl, S. A., Hariu, T. M., and Moore, W. S. (1989). Shelf sedimentation off the Ganges-Brahmaputra river system: evidence for sediment bypassing to the Bengal fan. *Geology*, 17:1132–1135.

Kuehl, S. A., Levy, B. M., Moore, W. S., and Allison, M. A. (1997). Subaqueous delta of the Ganges-Brahmaputra river system. *Marine Geology*, 144(1-3):81–96.

Kumar, S., Hazra, A., and Goswami, B. N. (2014). Role of interaction between dynamics, thermodynamics and cloud microphysics on summer monsoon precipitating clouds over the Myanmar Coast and the Western Ghats. *Climate dynamics*, 43:911–924.

Michael, N. A., Whittaker, A. C., and Allen, P. A. (2013). The Functioning of Sediment Routing Systems Using a Mass Balance Approach: Example from the Eocene of the Southern Pyrenees. *The Journal of Geology*, 121(6):581–606.

Michels, K. H., Kudrass, H. R., Hübscher, C., Suckow, A., and Wiedicke, M. (1998). The submarine delta of the Ganges-Brahmaputra: Cyclone-dominated sedimentation patterns. *Marine Geology*, 149(1-4):133–154.

Milliman, J. D. and Meade, R. H. (1983). World-wide Delivery of River Sediment to the Oceans. *The Journal of Geology*, 91(1):1–21.

Milliman, J. D. and Syvitski, J. P. M. (1992). Geomorphic/Tectonic Control of Sediment Discharge to the Ocean: The Importance of Small Mountainous Rivers. *Journal of Geology*, 100(5):525–544.

Morgan, J. P. and McIntire, W. G. (1959). Quaternary Geology of the Bengal Basin, East Pakistan and India. *Bulletin of the Geological Society of America*, 70(3):319–342.

Palamenghi, L., Schwenk, T., Spiess, V., and Kudrass, H. R. (2011). Seismostratigraphic analysis with centennial to decadal time resolution of the sediment sink in the Ganges-Brahmaputra subaqueous delta. *Continental Shelf Research*, 31(6):712–730.

Paola, C. and Martin, J. M. (2012). Mass-Balance Effects In Depositional Systems. *Journal of Sedimentary Research*, 82(6):435–450.

Paola, C. and Voller, V. R. (2005). A generalized Exner equation for sediment mass balance. *Journal of Geophysical Research: Earth Surface*, 110(F4):F04014.

Pate, R. D. (2008). *Multiple-proxy records of delta evolution and dispersal system behavior: fluvial and coastal borehole evidence from the Bengal Basin, Bangladesh*. PhD thesis, Vanderbilt University.

Pate, R. D., Goodbred, S. L., and Khan, S. R. (2009). Delta Double-Stack: Juxtaposed Holocene and Pleistocene Sequences from the Bengal Basin, Bangladesh. *Sedimentary Record*, 7(3):4–9.

Pethick, J. and Orford, J. D. (2013). Rapid rise in effective sea-level in southwest Bangladesh: Its causes and contemporary rates. *Global and Planetary Change*, 111:237–245.

Pickering, J. L., Goodbred, S. L., Beam, J. C., Ayers, J. C., Covey, A. K., Rajapara, H. M., and Singhvi, A. K. (2018). Terrace formation in the upper Bengal basin since the Middle Pleistocene: Brahmaputra fan delta construction during multiple highstands. *Basin Research*, 30:550–567.

Pickering, J. L., Goodbred, S. L., Reitz, M. D., Hartzog, T. R., Mondal, D. R., and Hossain, M. S. (2014). Late Quaternary sedimentary record and Holocene channel avulsions of the Jamuna and Old Brahmaputra River valleys in the upper Bengal delta plain. *Geomorphology*, 227:123–136.

Rahman, M. R. and Lateh, H. (2017). Climate change in Bangladesh: a spatio-temporal analysis and simulation of recent temperature and rainfall data using GIS and time series analysis model. *Theoretical and Applied Climatology*, 128(1-2):27–41.

Rashid, H., England, E., Thompson, L., and Polyak, L. (2011). Late glacial to Holocene Indian summer monsoon variability based upon sediment. *Terr. Atmos. Ocean. Sci*, 22(2):215–228.

Reitz, M. D., Pickering, J. L., Goodbred, S. L., Paola, C., Steckler, M. S., Seeber, L., and Akhter, S. H. (2015). Effects of tectonic deformation and sea level on river path selection: Theory and application to the Ganges-Brahmaputra-Meghna River Delta. *Journal of Geophysical Research: Earth Surface*, 120(4):671–689.

Renaud, F. G., Syvitski, J. P., Sebesvari, Z., Werners, S. E., Kremer, H., Kuenzer, C., Ramesh, R., Jeuken, A. D., and Friedrich, J. (2013). Tipping from the Holocene to the Anthropocene: How threatened are major world deltas? *Current Opinion in Environmental Sustainability*, 5(6):644–654.

Sandeep, K., Shankar, R., Warrier, A. K., Yadava, M. G., Ramesh, R., Jani, R. A., Weijian, Z., and Xuefeng, L. (2017). A multi-proxy lake sediment record of Indian summer monsoon variability during the Holocene in southern India. *Palaeogeography, Palaeoclimatology, Palaeoecology*, 476(March):1–14.

Sarkar, A., Sengupta, S., McArthur, J. M., Ravenscroft, P., Bera, M. K., Bhushan, R., Samanta, A., and Agrawal, S. (2009). Evolution of Ganges-Brahmaputra western delta plain: Clues from sedimentology and carbon isotopes. *Quaternary Science Reviews*, 28(25-26):2564–2581.

Sincavage, R., Goodbred, S., and Pickering, J. (2018). Holocene Brahmaputra River path selection and variable sediment bypass as indicators of fluctuating hydrologic and climate conditions in Sylhet Basin, Bangladesh. *Basin Research*, 30(2):302–320.

Singh, S. K. and France-Lanord, C. (2002). Tracing the distribution of erosion in the Brahmaputra watershed from isotopic compositions of stream sediments. *Earth and Planetary Science Letters*, 202(3-4):645–662.

SMRC (2003). The Vulnerability Assessment of the SAARC Coastal Region due to Sea Level Rise: Bangladesh Case. Technical report, SAARC Meteorological Research Center, Dhaka. SMRC-No. 3.

Strong, N., Sheets, B., Hickson, T., and Paola, C. (2005). A mass-balance framework for quantifying downstream changes in fluvial architecture. *Spec. Publs int. Ass. Sediment.*, 35:243–253.

Syvitski, J. P. M., Kettner, A. J., Overeem, I., Hutton, E. W. H., Hannon, M. T., Brakenridge, G. R., Day, J., Vörösmarty, C., Saito, Y., Giosan, L., and Nicholls, R. J. (2009). Sinking deltas due to human activities. *Nature Geoscience*, 2(10):681–686.

Taylor, M., Stevens, J., and Rocchio, L. (2018). Nasa Earth Observatory: The Sculpting of the Ebro Delta.

Turner, A. G. and Annamalai, H. (2012). Climate change and the South Asian summer monsoon. *Nature Climate Change*, 2:587.

Umitsu, M. (1993). Late quaternary sedimentary environments and landforms in the Ganges Delta. *Sedimentary Geology*, 83(3):177–186.

Umitsu, M. (2014). Late Quaternary Sedimentary Environment and Landform Evolution in the Bengal Lowland. *Geographical review of Japan, Series B.*, 60(2):164–178.

Whitehead, P. G., Barbour, E., Futter, M. N., Sarkar, S., Rodda, H., Caesar, J., Butterfield, D., Jin, L., Sinha, R., Nicholls, R., and Salehin, M. (2015). Impacts of climate change and socio-economic scenarios on flow and water quality of the Ganges, Brahmaputra and Meghna (GBM) river systems: Low flow and flood statistics. *Environmental Sciences: Processes and Impacts*, 17(6):1057–1069.

Wilson, C. A. and Goodbred Jr., S. L. (2015). Construction and Maintenance of the Ganges-Brahmaputra-Meghna Delta: Linking Process, Morphology, and Stratigraphy. *Annual Review of Marine Science*, 7(1):67–88.

Zhisheng, A., Kutzbatch, J. E., Prell, W. L., and Porter, S. C. (2001). Evolution of Asian monsoons and phased uplift of the Himalaya-Tibetan plateau since Late Miocene times. *Nature*, 411(6833):62–66.